Fuel 310 (2022) 122145

Contents lists available at ScienceDirect

Fuel

journal homepage: www.elsevier.com/locate/fuel

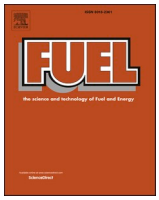

Full Length Article

Chemical study of bottom ash sintering in combustion of pelletized residual agricultural biomass

Javier Royo *, Paula Canalís, David Quintana

University of Zaragoza, c/María de Luna 3, E-50018 Zaragoza, Spain

ARTICLE INFO

Keywords:
Biomass combustion
Agropellet
Fixed bed reactor
Bottom ash sintering
SEM-EDS
P-XRD

ABSTRACT

Although residual agricultural biomass is a high-potential energy source, its use is curtailed by the characteristics of its ash (quantity and composition). This ash can cause problems during combustion, including bottom ash sintering, which is the main focus of this study. Results of bottom ash proportion and sintering degree yielded by combustion tests carried out with four different agropellets (one was exclusively woody, and the others were blended with various herbaceous components –mixed agropellets) under different operating conditions in a laboratory fixed-grate reactor were presented in a previous paper. The inlet air temperature and the excess air were the two controlled operating parameters in the tests. To bring the analysis further, samples of bottom ash collected during these tests have been characterized using SEM-EDS and P-XRD techniques. The results confirmed that, given its high content of alkali metals and its high ratio (K+Na)/(Si+P), the differences in sintering behavior presented by the four agropellets are related to the formation of alkali metal silicates and phosphates; Si+P is the limiting and determining content that condition the sintering severity. Regarding the influence of operating conditions, only small variations in the composition of both the sintered and not sintered fractions of the bottom ash have been detected when varying inlet air temperature and excess air in the analyzed range. Nevertheless, these SEM-EDS results have led to the detection of two opposing phenomena related to increased excess air: higher ash entrainment and lower vaporization, which are associated with the increase of air velocity and the reduction of combustion temperature, respectively. Whereas in the mixed agropellets and in the range of excess air tested these two effects offset each other, woody agropellet is significantly affected by entrainment due to its lack of sintered matter. These results provide useful information towards a solution of the problem posed by sintering in the combustion of residual agricultural biomass.

1. Introduction

Mid-term forecasts concerning the new uses of forest biomass (e.g., biorefineries and new materials) will hinder the recently increased use of this resource in energy production [1,2]. Therefore, in order to meet EU targets for the contribution of biomass to the heating and cooling sector, the use of biomass from the agricultural sector must be taken into consideration [3].

Among these new resources, herbaceous crop residues stand out for their potential. However, in order for the use of these fuels to become widespread, the problems associated with the thermal conversion of this type of biomass (sintering, deposition, corrosion, erosion and emissions) need to be overcome. These problems are essentially due to the characteristics of its ash (quantity and composition). Research undertaken in recent decades has pointed out the critical influence of the chemical composition of ash [4-21], especially the concentration of Na, Mg, Al, Si, P, S, Cl, K and Ca [5]. Ash-forming elements include those added by anthropogenic activities (such as harvesting or processing) [22,23]

Abbreviations: %m/m, mass percentage; d.b, dry basis; EDS, Energy Dispersive X-ray Spectrometry; HHV, High heating value ($MJ{\cdot}kg^{-1}$); LHV, Low heating value ($MJ{\cdot}kg^{-1}$); PV, Vineyard pruning agropellet; PVB, Vineyard pruning and Barley straw mixed agropellets; PVC, Vineyard pruning and Corn stover mixed agropellets; PVCB, Vineyard pruning, Corn stover and Barley straw mixed agropellets; P-XRD, Powder X-ray Diffractometry; S1, Bottom ash fraction not sintered; S2/3, Fraction S2 plus fraction S3; S2, Bottom ash fraction with a low sintering status; S3, Bottom ash fraction with a high sintering status; SEM, Scanning Electron Microscopy; Ta, Inlet air temperature (°C); TC3m, Mean flame temperature (°C); TCi, Temperature registered by the thermocouple located in position i; w.b, wet basis; XS, Crystallite size; λ, Excess air ratio.

* Corresponding author.
E-mail address: fjroyo@unizar.es (J. Royo).

https://doi.org/10.1016/j.fuel.2021.122145
Received 7 May 2021; Received in revised form 3 September 2021; Accepted 28 September 2021
Available online 23 November 2021

which can contaminate the biomass, although these elements are typically less reactive [5].

During combustion, ash undergoes physical and chemical transformations that lead to fractionation. One part, mainly related to alkali metal compounds, is volatilized. After complex and not always well known mechanisms [5,24,25], these compounds can directly condense or, after forming aerosols, be deposited by thermophoresis and/or turbulent diffusion [5,25–27] on the heat-exchange surfaces of the equipment. Ash entrainment of solid particles (coarse fly ash) in the gas-combustion flow from the bed can also ensue and, in given conditions, these particles can be deposited on exchange surfaces by inertial impact. These phenomena (volatilization and ash entrainment) can also be responsible, besides deposition, for both corrosion and erosion, which reduce the performance and lifetime of the equipment [28,29].

Other part of the components of the ash forms a solid fraction which accumulates in the grate (bottom ash). Under certain combustion conditions and when the fuel ash fusion temperatures are sufficiently low, the bottom ash can sinter and cause severe problems in the equipment, affecting conversion in the bed, restricting the effectivity of the grate and negatively affecting gas emission control [4,28–31]. The main phenomenon in the process of sintering is the formation of low-melting alkali metal silicates, mainly K, with which other elements such as alkaline earth metals (mainly Ca and Mg) can subsequently interact [5]. The eutectic temperatures of the K_2O-SiO_2 system, which can be as low as 600 °C [5], are a critical factor in this phenomenon. Bottom ash sintering through this mechanism is especially acute in herbaceous fuels compared to woody biomass, since its ash content is generally higher, as well as its concentration of Si and K [23]. Phosphorus has also a key role in sintering as it can form alkali phosphates (P dominates over Si [32]), which also have low melting temperatures [32]. However, in agricultural biomass P is considerably lower than Si [33], but not negligible.

Taking into account these characteristics of herbaceous biomass, the mix of herbaceous and woody fuels, among other strategies, may reduce the above-mentioned problems. The objective of these blends is to both decrease ash percentage in the fuel and improve its composition. Regarding the latter, the aim is to reduce or dilute the conflicting elements (such as K, Cl, S and N) and/or obtain molar ratios between elements that diminish the problems of sintering, deposition and gaseous emissions [4,19,35–37]. This paper shows the results and analysis of tests carried out with blends of three types of residual agricultural biomass: two herbaceous (barley straw and corn stover) and one woody (vineyard pruning).

In addition to the influence of the chemical composition of ash, combustion conditions on the bed, both design- and operation-related, and their impact on problems associated with thermal conversion has been also researched [16,17,38–41]. In order to analyze the influence of all these factors it is essential to carry out combustion tests. Due to the complexity of the phenomena involved in the ash fractionation, these tests are frequently undertaken in laboratory reactors (most of which operate fixed-grate technology) so that adequate control over combustion conditions is maintained [11,16,42–51].

In a previous study [52], various aspects related to combustion (reactivity, bottom ash quantity, sintering degree and deposition rate) were examined for different pellets made of residual agricultural biomass and evaluated under different operating conditions in a laboratory fixed-grate reactor. Based on the tests carried out in that study, it was established that both the velocity of the ignition front (and therefore the ignition rate) and the combustion temperature achieved were adequate for a very wide range of excess air ratio (λ). However, the differences in behavior in terms of sintering between the fuels could not be satisfactorily explained; nor was it possible to determine why the quantity of bottom ash remained almost constant for the fuels with an herbaceous component as λ increased.

The following step in the analysis, presented in this paper, intends to delve into these aspects by characterizing the bottom ash samples collected during the tests. Scanning Electron Microscopy (SEM) with Energy Dispersive X-ray Spectrometry (EDS) was used to know their elementary composition and Powder X-ray Diffractometry (P-XRD) was used to determine the main phases formed within the ash.

Based on this information, compositional differences between the most and least sintered fraction identified in the bottom ash for each fuel, as well as between fuels, were analyzed and related to the sintering degree and to the composition of the ash fuel preliminary analysis.

Additionally, by using the information obtained from SEM-EDS together with the quantity of ash collected in each test, it is possible to analyze the influence of operating conditions (inlet air temperature and excess air) in bottom ash behavior and to identify how volatilization and ash entrainment were affected by these factors.

Against this background, the aim of this study is to advance in the knowledge of the sintering phenomenon, and contribute to find solutions to the problems it poses and, therefore, to achieve the desired increase in the use of residual agricultural biomass in the domestic sector.

2. Material and methods

2.1. Fuels

Three agricultural residual biomasses (two herbaceous and one woody) were selected owing to their wide availability in both Europe and the rest of the world: vineyard pruning, barley straw and corn stover. The energy potential of these biomasses can be estimated at over 500 PJ/yr for the EU (see [53]).

Given these raw materials, four agropellets were produced:

- Woody agropellet: 100% Vineyard pruning (PV)[1]
- Mixed agropellets (Vineyard pruning blended with an herbaceous component, percentages in mass basis as received):
  - o 70% Vineyard pruning + 30% Barley straw (PVB)
  - o 70% Vineyard pruning + 30% Corn stover (PVC)
  - o 60% Vineyard pruning + 20% Corn stover + 20% Barley straw (PVCB)

The three mixed agropellets were designed to meet the requirements of the ISO 17225–6:2014 standard for non woody pellets, both A class (PVB) and B class (PVC and PVCB), the limiting parameters being the ash and Cl contents. Pellets produced had a diameter of 6.5 mm with lengths ranging from 10 to 30 mm. More information about the fuel design process followed can be found in [54].

The main thermochemical properties of the four fuels used are reproduced from [52] and presented in Tables 1 and 2.

2.2. Reactor

As noted, when investigating ash phenomena during combustion it is usual to resort to laboratory reactors. In the case of fixed bed reactors, simplified geometries are generally used to be able to consider one-dimensional behavior [49].

In order to perform the combustion tests of this study, an experimental fixed-grate reactor was used (see Fig. 1). In this batch-fed reactor, inlet air is injected through the grate from the bottom by means of a fan equipped with a variable-frequency drive which allows airflow to be regulated. Since experiments require inlet air temperature (Ta) to remain under control, the reactor is equipped with a refrigerator and an electrical resistor either to cool or heat the air as needed. It allowed two different types of tests to be undertaken: without preheating (inlet air at 25 °C) and with preheating (inlet air at 80 °C).

The reactor is fitted with 15 N-thermocouples to monitor temperature at both the bed and the freeboard. They take measurements from

[1] Vineyard pruning residues used to produce this agropellet were not the same as those used for the mixed agropellets.

Table 1
Agropellets properties.

		PV Vineyard pruning 100%	PVB Barley straw 30%	PVC Corn stover 30%	PVCB Corn stover 15% Barley straw 15%
Bulk density (kg·m^{-3})[a]		599	562	556	546
Proximate analysis (% m/m d.b)	Volatile matter[b]	76.5	72.4	72.1	72.3
	Fixed carbon[c]	20.5	21.7	18.6	21.2
	Ash[d]	3.1	5.9	9.3	6.5
Total moisture (% m/m w. b.)[e]		9.0	9.1	9.2	9.0
Ultimate analysis (% m/m d.b.)	Carbon[f]	48.9	46.36	46.01	46.36
	Hydrogen[f]	5.8	5.77	5.64	5.55
	Nitrogen[f]	0.55	0.56	0.55	0.60
	Sulfur[g]	0.09	0.055	0.050	0.094
	Chlorine[g]	0.03	0.047	0.080	0.090
	Oxygen[c]	41.6	41.29	38.33	40.58
HHV (d.b. at p=constant) (MJ·kg^{-1})[h]		19.11	18.54	18.06	18.36
LHV (w.b. at p=constant) (MJ·kg^{-1})[h]		16.01	15.48	15.06	15.40

[a]EN 15103:2009 [b]EN-ISO 18123:2016 [c]Calculated [d]EN-ISO 18122:2016 [e]EN-ISO 18134:2016
[f]EN-ISO 16948:2015 [g]EN-ISO 16994:2015 [h]EN-ISO 14918:2011

Table 2
Ash properties.

		PV	PVB	PVC	PVCB
Chemical ash composition (% m/m d.b.)[a]	Al_2O_3	0.91	2.72	2.19	2.30
	CaO	42.39	45.77	48.17	40.54
	Fe_2O_3	0.71	2.22	1.98	1.27
	K_2O	30.09	14.88	15.79	19.43
	MgO	10.45	8.64	7.64	11.01
	Na_2O	0.62	0.41	0.39	0.38
	P_2O_5	7.35	4.45	4.00	4.36
	SO_3	3.95	2.32	3.24	4.39
	SiO_2	2.65	17.70	15.31	15.22
	TiO_2	0.07	0.17	0.18	0.16
	Cl	0.12	0.21	0.57	0.54
Ash melting temperatures under oxidizing conditions (°C)[b]	Initial deformation temperature	1240	1130	1310	1330
	Hemisphere temperature	>1500	1310	1460	1460
	Flow temperature	>1500	1370	1480	1470

[a] EN-ISO 16967:2015 [b]CEN/TS 15370-1:2006

the center of the combustion chamber and are aligned. For identification purposes, they are numbered from TC1, the closest to the grate, to TC15, located in the upper part of the reactor. Based on the recorded temperatures, it is possible to estimate the mean flame temperature (TC3m, °C) as the average value of the temperature registered by TC3 in the interval between TC2 and TC1 reaching 500 °C. For more details about reactor characteristics, operation and regulations see [52].

2.3. Ash analysis

Once combustion was completed and the reactor cooled down, bottom ash was collected from the surface of the grate for weighing and classification, which allowed the tendency of each fuel to sinter to be determined [14,28,33,35,55]. Bottom ash proportion was calculated as

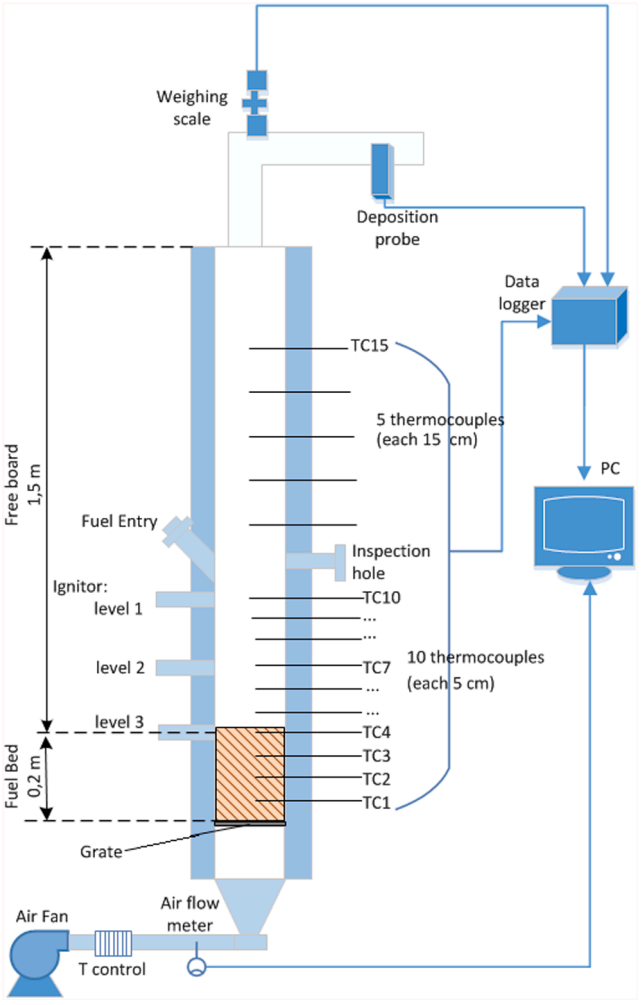

Fig. 1. Diagram of the experimental test facility [52]

the total mass of ash collected compared to the total mass of ash introduced with the fuel. The following categories, based on a revised classification of sintering statuses established in previous works [14,33], were used: S1, ash which passes through a 3.15 mm sieve and was considered not to be sintered; S2, ash which does not pass through a 3.15 mm sieve, but was easily disaggregated by hand pressure, indicative of low sintering status; and S3, ash which does not pass the 3.15 mm sieve, and was difficult to disaggregate by hand pressure, which is indicative of high sintering status. Since the difference between S2 and S3 was subjective, both were regarded as a single category (S2/3). The sintering degree of a fuel was calculated as the percentage of this last fraction (S2/3) compared to the total ash introduced with the fuel in each test. The higher this percentage, the more problematic the fuel is considered.

For all tests, samples of S1 and S2/3 bottom ash fraction were collected. SEM-EDS and P-XRD methods were used to characterize the bottom ash samples. These complementary techniques are the most widely used for the identification and characterization of ash compounds [19,27,29,56–61].

The samples were crushed in a mortar to obtain a homogeneous mixture with an adequate particle size for analysis. Each sample was glued onto metal plates with carbon tape and then coated with carbon before being analyzed by SEM-EDS. The equipment used was a Carl Zeiss Merlin electronic field emission microscope equipped with Gemini Column, with acceleration voltages between 0.02 and 30 kV, fitted with an EDS X-MAS detector by Oxford Instruments with a window of 20 mm^2 and energy resolution between 127 eV and 5.9 keV. For each sample,

three 1-mm^2 representative zones were selected using the angle selective backscattered electron detector (AsB). Average elemental composition was obtained through EDS, using a voltage of 15 kV. INCA software was used to process the results. Major participating elements in the most important ash transformation processes – namely Na, Mg, Al, Si, P, S, Cl, K, Ca and Fe – were included in the analysis.

In addition, four combustion experiments without preheating were undertaken for each fuel. These tests were chosen to evenly cover the range of λ for each fuel (see Table 3). An experiment with preheating was also selected for each agropellet, all of which presented an almost-identical excess air ratio value (λ≈1.3). In all instances, the crystalline matter composition of the S1 and S2/3 bottom ash samples was determined by P-XRD. Standard X-ray diffraction patterns were collected at room temperature using a Rigaku D/max instrument with a copper rotating anode and a graphite monochromator to select CuKα wavelength. The measurements were performed at 40 kV and 80 mA, in the angular range from 5° to 80° on 2θ, applying a step size of 0.03° and a counting rate of 1 s/step. X-ray patterns were analyzed with JADE 7 software, with access to the JCPDS-International Centre for Diffraction Database (2000) and profile-based RIR analysis. In addition to this, peak decomposition was carried out through profile fitting, using a pseudo-Voigt approximation. The crystallite size of each peak (XS) was measured and the proportion of the amorphous phase was calculated, considering peaks with an XS below 80 Å to be included.

2.4. Test features

A total of 68 combustion tests were carried out with the four fuels; all tests followed the same protocol. Detailed information about this experimental protocol can be found in [52]. As noted above, tests both with and without preheating (the former are referred to as "ph" experiments) were undertaken with different inlet air temperatures. Table 3 summarizes the main features of the experiments performed.

The λ value used was greater than 1 in all tests (over-stoichiometric conditions) to reproduce combustion conditions in typical small domestic equipment with a primary λ>1. As a result, values of inlet air flow in the order of magnitude of those used in this domestic equipment and similar to those presented by other authors (e.g., [49] in his tests with λ>1) were obtained.

2.5. Statistical analysis

In order to determine the goodness of the linear correlations shown in section 3, a statistical analysis through the estimation of Pearson's correlation coefficient (r) and its corresponding p-value (p) was undertaken. A correlation is considered statistically significant when p<.05, although all numerical values of p<.1 are included.

3. Results and discussion

3.1. SEM-EDS and P-XRD results

Table 4 and 5 present mean values and range (minimum and maximum values) of elemental composition yielded by SEM-EDS for each of the four fuels (S1 and S2/3 fractions), expressed as a percentage of the total mass of measured elements (Na, Mg, Al, Si, P, S, Cl, K, Ca and Fe).

Fig. 2 and Fig. 3 plot the values summarized in Table 4 and 5 against λ, omitting the elements with a mean concentration lower than 5% (Al, S, Cl and Fe). Due to their chemical similarity and the almost-identical roles they play in the reactions that take place in ash transformation processes, the concentrations of K and Na [5], as well as Ca and Mg [62], are aggregated in both figures.

Table 6 and 7 present the crystalline phases and amorphous concentrations of S1 and S2/3 fractions of the five selected tests per fuel using P-XRD.

3.2. Discussion

3.2.1. Fuel comparison

Based on previously published results [52,53], the important quantitative differences between the mixed agropellets and PV in terms of sintering behavior must be highlighted. As shown in Table 3, mean bottom ash proportion for PV was relatively low (25% maximum), while for the mixed agropellets it was much higher (in the order of 50–75%). Concerning the mean sintering degree, again the two types of fuels behaved differently (Table 3): it was under 2% for PV, and between 34 and 58% for mixed agropellets.

As noted, in contrast to bottom ash, part of the fuel ash can leave the bed by vaporization, mainly in form of alkali chlorides, hydroxides and sulfates; another part can do it by entrainment. In relation to this entrainment, since the fuels which showed a greater sintering degree also presented higher bottom ash proportion values, a clear relationship is attested between both parameters. The reason for this could be that a high sintering degree precludes particle entrainment [52].

The differences attested in bottom ash fractions left by the different fuels tested were not only quantitative, as revealed by the visual and tactile examination of the ashes (see Fig. 4). The molten compounds

Table 3
Outline of test features.

		Without preheating tests (Ta = 25 °C)				Preheated tests (Ta = 80 °C)			
Fuel		**PV**	**PVB**	**PVC**	**PVCB**	**PV**	**PVB**	**PVC**	**PVCB**
Number of tests performed		10	10	10	12	8	6	6	6
Fed fuel (kg)		4.03	3.78	3.74	3.67	4.03	3.78	3.74	3.67
λ	**Mean**	1.52	1.61	1.67	1.59	1.46	1.59	1.35	1.41
	Range (Min.-Max.)	1.15–2.04	1.24–2.30	1.18–2.29	1.23–2.07	1.27–1.65	1.21–2.14	1.26–1.54	1.28–1.51
Inlet air flow ($kg{\cdot}m^{-2}{\cdot}s^{-1}$)[a]	**Mean**	0.42	0.42	0.44	0.42	0.49	0.50	0.50	0.48
	Range (Min.-Max.)	0.36–0.47	0.38–0.48	0.41–0.47	0.37–0.45	0.43–0.52	0.46–0.54	0.49–0.54	0.46–0.51
Air Velocity ($m{\cdot}s^{-1}$)[b]	**Mean (all tests)**	8.0	8.1	8.4	8.0	11.0	11.2	11.6	11.0
	Range (Min.-Max.)	6.9–9.1	7.2–9.1	7.9–9.0	7.1–8.5	9.9–11.9	10.4–12.2	10.7–12.3	10.5–11.7
	Mean (only tests within similar λ range than ph tests)	7.9	8.0	8.3	7.8	—	—	—	—
TC3m (°C)	**Mean (all tests)**	1013	963	958	952	925	1004	1024	1029
	Range (Min.-Max.)	894–1109	783–1079	778–1074	808–1056	846–1038	913–1084	984–1058	1013–1052
	Mean (only tests within similar λ range than ph tests)	1026	983	1006	1001	—	—	—	—
Bottom ash proportion (%)	**Mean**	25.3	74.7	50.0	59.5	13.0	71.2	47.7	55.9
Sintering degree (%)	**Mean**	1.6	51.8	33.8	40.1	0.6	57.5	40.2	45.9

[a] air mass flow by unit area of the grate [b] air velocity through the holes of the grate

Table 4
Mean values (range) of the elemental composition (SEM-EDS) of S1 fraction of bottom ash expressed as a percentage of the total mass of measured elements – Na, Mg, Al, Si, P, S, Cl, K, Ca and Fe.

SEM-EDS analysis results (%m/m)								
	Without preheating tests (Ta = 25 °C)				Preheated tests (Ta = 80 °C)			
	PV	PVB	PVC	PVCB	PV	PVB	PVC	PVCB
Na	0.33 (0.25–0.42)	0.24 (0.12–0.32)	0.14 (0.05–0.24)	0.22 (0.15–0.32)	0.34 (0.3–0.37)	0.21 (0.17–0.24)	0.15 (0.11–0.22)	0.2 (0.13–0.32)
Mg	8.27 (7.44–9)	4.83 (4.54–5.22)	4.75 (3.13–5.64)	5.25 (3.82–5.94)	7.4 (6.17–7.96)	4.46 (4.11–4.87)	4.52 (3.96–4.95)	4.68 (4.21–5.39)
Al	0.6 (0.47–0.7)	1.63 (1.43–1.86)	1.59 (1.37–2)	1.63 (1.43–1.86)	0.59 (0.48–0.76)	1.56 (1.25–1.8)	1.52 (1.36–1.69)	1.48 (1.32–1.59)
Si	2.41 (1.79–3.62)	11.23 (8.66–13.52)	12.28 (8.39–18.08)	13.52 (10.34–17.15)	2.86 (1.51–4.33)	12.59 (11.47–13.45)	13.74 (11.43–17.51)	14.16 (11.59–18.44)
P	5.52 (4.95–6.21)	2.65 (2.32–2.83)	2.06 (1.11–2.59)	2.64 (1.87–3.03)	5 (4.13–5.43)	2.51 (2.29–2.75)	2.15 (1.83–2.5)	2.39 (2.02–2.87)
S	1.3 (0.76–1.56)	1.38 (1.14–1.89)	0.87 (0.57–1.07)	1.69 (1.36–1.97)	1.45 (1.35–1.62)	1.16 (1.03–1.32)	0.78 (0.55–0.92)	1.28 (0.92–1.64)
Cl	0.12 (0.06–0.15)	0.97 (0.64–1.49)	0.83 (0.52–1.2)	0.69 (0.06–0.97)	0.1 (0.02–0.2)	0.67 (0.46–1.01)	0.73 (0.46–0.9)	0.52 (0.32–0.84)
K	28.29 (16.92–34.98)	24.29 (21.48–29.65)	12.31 (7.94–15.91)	19.55 (14.07–22.46)	31.13 (24.23–34.3)	22.48 (20.67–25.77)	13.55 (11.15–15.25)	18.1 (15.85–22.3)
Ca	52.07 (46.78–61.86)	50.69 (45.14–55.86)	63.69 (59.56–68.5)	53.31 (49.67–58.67)	50.14 (47.27–56.7)	52.2 (48.46–53.57)	61.46 (58.36–66.57)	55.92 (50.76–60.25)
Fe	1.08 (0.71–1.68)	2.09 (1.76–2.73)	1.48 (1.23–1.84)	1.52 (1.19–2.23)	1 (0.63–2.16)	2.16 (1.62–2.53)	1.4 (1.23–1.6)	1.27 (1.19–1.34)

Table 5
Mean values (range) of the elemental composition (SEM-EDS) of S2/3 fraction of bottom ash expressed as a percentage of the total mass of measured elements – Na, Mg, Al, Si, P, S, Cl, K, Ca and Fe.

SEM-EDS analysis results (%m/m)								
	Without preheating tests (Ta = 25 °C)				Preheated tests (Ta = 80 °C)			
	PV	PVB	PVC	PVCB	PV	PVB	PVC	PVCB
Na	0.1 (0–0.25)	0.19 (0.09–0.3)	0.17 (0.07–0.22)	0.23 (0.14–0.3)	0.2 (0.07–0.36)	0.2 (0.13–0.25)	0.18 (0.1–0.22)	0.22 (0.17–0.27)
Mg	9.78 (5.58–12.37)	3.5 (2.49–4.19)	4.02 (2.84–4.86)	4.49 (3.86–5.08)	6.17 (2.43–10.08)	3.53 (3.14–3.91)	4.08 (3.49–4.34)	4.51 (4.19–4.89)
Al	1.09 (0.9–1.25)	1.46 (1.15–1.81)	1.51 (1.15–1.81)	1.6 (1.43–1.79)	1.33 (0.66–3.02)	1.47 (1.29–1.65)	1.65 (1.56–1.79)	1.71 (1.58–1.83)
Si	7.43 (3.47–18.51)	18.6 (13.27–23.93)	20.71 (15.14–24.83)	19.9 (14.43–24.31)	11.98 (2.72–24.02)	19.58 (17.38–21.47)	23.38 (21.98–26.06)	22.18 (20.03–24.76)
P	5.82 (2.97–7.56)	1.78 (1.13–2.14)	1.55 (1.07–2.06)	1.99 (1.68–2.35)	3.64 (1.39–6.24)	1.83 (1.59–2.11)	1.51 (1.16–1.76)	2.05 (1.91–2.15)
S	0.38 (0.11–0.74)	0.93 (0.25–2.22)	0.4 (0.09–1.89)	1.27 (0.15–3.14)	0.62 (0.22–2.05)	0.44 (0.22–0.64)	0.11 (0.04–0.17)	0.39 (0.19–0.57)
Cl	0.02 (0–0.08)	0.06 (0–0.19)	0.05 (0–0.12)	0.1 (0–0.86)	0.01 (0–0.05)	0.04 (0–0.1)	0.01 (0–0.03)	0.01 (0–0.05)
K	4.7 (1.06–10.87)	15.17 (9.49–17.89)	7.71 (6.13–9.64)	13.99 (10.75–18.76)	13.08 (6.7–20.14)	14.66 (12.31–18.02)	7.91 (6.62–9.32)	11.82 (10.3–13.38)
Ca	68.75 (56.37–73.02)	55.91 (49.65–69.74)	62.39 (55.97–71.78)	54.78 (49.07–61.62)	60.7 (51.26–65.39)	56.07 (53–60.65)	59.64 (56.45–62.02)	55.49 (52.66–58.31)
Fe	1.95 (0.99–3.7)	2.4 (1.91–3.18)	1.49 (1.14–1.84)	1.67 (1.09–2.63)	2.28 (0.81–6.2)	2.19 (1.88–2.54)	1.55 (1.34–1.7)	1.64 (1.37–1.83)

merged with ash particles that are not molten, forming ash blocks of various sizes. In the mixed agropellets (Fig. 4-b) large and hard structures typical of silicate melting were found in the S2/3 fraction, while the structures found after PV tests (Fig. 4-a) were less consistent. Important differences were also attested in the S1 fraction: for PV, a large quantity of ash in the form of fine dust was found, whereas in the mixed agropellets the quantity of S1 fraction was smaller and generally less fine and even contained some ash blocks, which, despite being partially melted, were small enough to be classed as S1 fraction according to the classification criteria applied (these differences are not clearly visible in Fig. 4).

SEM-EDS (Table 4 and 5, and Figs. 2 and 3) and P-XRD (Table 6 and 7) were used to try to understand these differences in behavior.

First, amorphous fraction contents range from 3 to 32% (Table 6 and 7). As noted by some authors (e.g., [63]), although a significant proportion of the melted ash is found in amorphous form (i.e. with a low degree of crystallinity, based on the crystallite size established above), there are some phases that, after the ash has melted, can recrystallize, and be detected by P-XRD. Along with the sintering-related compounds that can be present in the amorphous phase (mainly K-silicates), other components – e.g. organic matter –could also be detected in this fraction [34].

3.2.1.1. Alkaline earth metals (Ca and Mg). The results show that the Ca+Mg group is the most abundant in the bottom ash by far, amounting to more than 50% in all fractions and fuels, and no major differences are attested between fuels: although PV presents a higher percentage than the rest in the S2/3 fraction, owing to the low percentage that this fraction represents (see Table 3) this is not regarded as overly relevant. However, P-XRD results indicate that significant differences exist (across both fractions and fuels) in the phases formed by these elements. In S1 fraction (Table 6), alkaline earth metals compounds are the most abundant in all fuels and conditions: carbonates are dominant, mainly $CaCO_3$ (calcite), although $K_2Ca(CO_3)_2$ is also attested (as fairchildite and

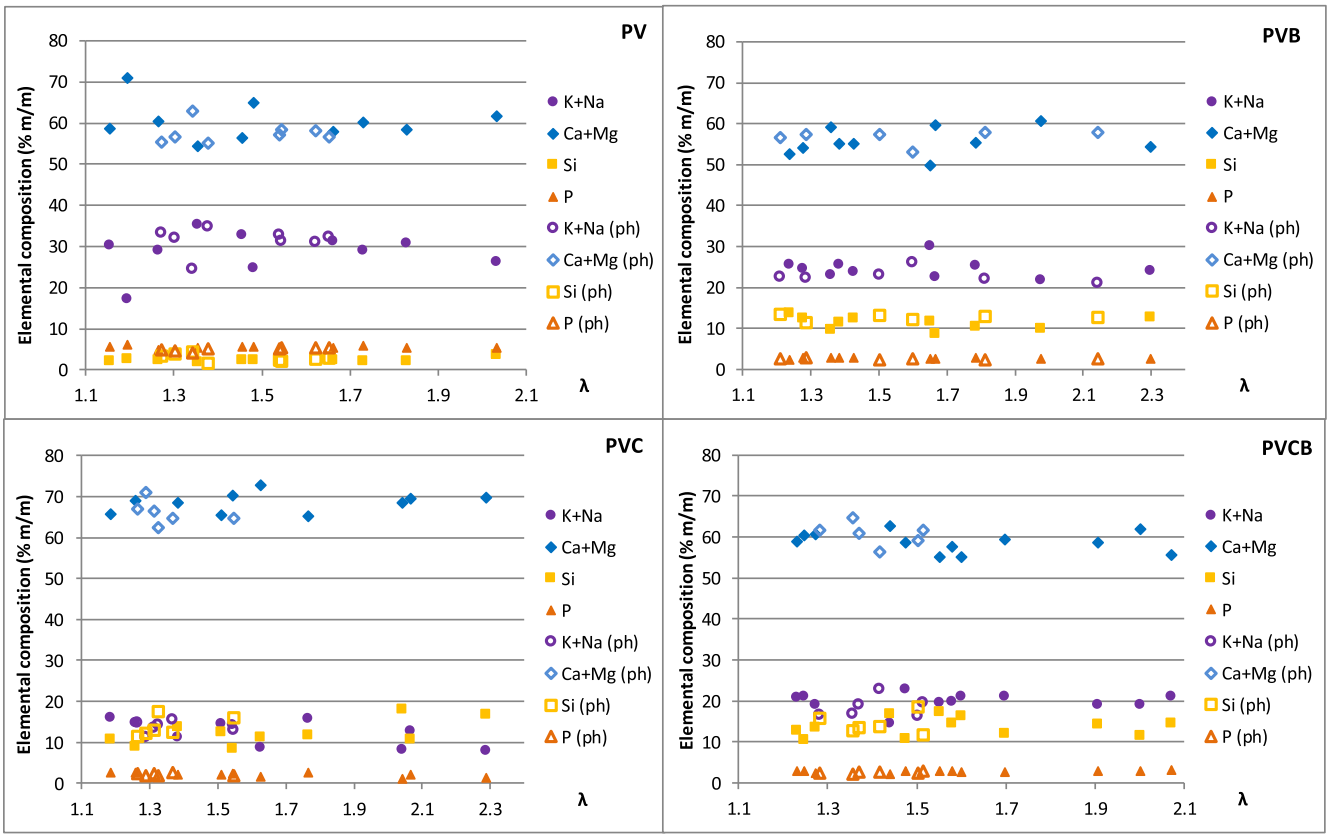

Fig. 2. Elemental composition (SEM-EDS) of S1 fraction of bottom ash expressed as the percentage of the total mass of measured elements (Na, Mg, Al, Si, P, S, Cl, K, Ca and Fe) against excess air ratio (λ) for PV, PVB, PVC and PVCB. Tests with (ph) and without inlet air preheating.

butschliite). Both of these compounds are very common in biomass ash [5], especially in fuel ash with a high proportion of Ca (i.e. the fuels used in this study), and are generated in areas of relatively low temperatures [5]. Therefore, they were either formed in specific low temperature areas or during the cooling process after combustion [17]. In fraction S2/3 (Table 7) alkaline earth metal silicates (Ca_2SiO_4, $Ca_3Mg(SiO_4)$ and $Ca_2Mg(Si_2O_7)$) are clearly predominant in the crystalline phase of the mixed agropellets, amounting to over 80% of this phase. This difference is significant since in S1 fraction alkaline earth silicates rarely exceed 10%. Moreover, this is another major difference with PV, which does not present these compounds in the S1 fraction, and on average they fall short of 30% in the S2/3 fraction, far below the values detected in the mixed agropellets. As for the remaining phases, the notable reduction of $CaCO_3$ in S2/3 fraction in all fuels stands out. Another difference between PV and the mixed agropellets lies in the high content of alkaline earth metal oxides in PV ash, both in the S1 and S2/3 fractions (around 20 and 40% of the crystalline part, respectively), especially MgO. This compound presents lower reactivity compared to CaO [5,26,64]; as there is less Si with which to react in PV, Mg tends to remain in oxide form. The high content of alkaline earth metal oxides could explain the relative brittleness observed in PV ash (Fig. 4), as their high melting temperatures [5,65] does not exacerbate bottom ash sintering.

3.2.1.2. Alkali metals (K and Na). The alkali metal group K+Na presents the second highest concentration in S1 in nearly every case (Table 4 and Fig. 2), where values in the order of 30% are found for PV, 25% for PVB, 20% for PVCB and 13% for PVC. In S2/3, the percentage of K+Na detected by SEM-EDS is considerably lower in all cases (up to 5%, 15%, 13% and 9% in PV, PVB, PVCB and PVC respectively) (Table 5 and Fig. 3). One possible explanation is their partial displacement by alkaline earth metals when, after the initial formation of the K and Na silicates that melt at relatively low temperatures, these compounds react with Ca and Mg (dissolution and precipitation), with which they have great thermodynamic affinity [5,33]. Although it is true that the origin of the Ca-(Mg)-silicates detected by P-XRD can vary (mainly secondary origin, with different formation routes [63]), this is one of the possible ways they can form. For this reason, the presence of these secondary compounds in these concentrations can be representative of the sintering of the mixed fuels.

Continuing with the P-XRD results, it should be noted that in S1 fraction, K is detected only in the form of $K_2Ca(CO_3)_2$ (Table 6), its concentration being especially significant in PV (more than 18%) due to the low proportion of Si+P in this fuel, which prevents the formation of large amounts of alkali metal silicates and phosphates with a tendency to sinter. In the case of S2/3 fraction, K is detected only in PVB forming KCl, which could be related to their retention as gas within the solid, as in [66]. This virtual absence of K-containing crystalline phases, in both the S1 and the S2/3 fraction, should be highlighted, mainly because it must be present in the amorphous material, predictably forming silicates and phosphates.

3.2.1.3. Silicon. Si is the element in which greater differences in terms of concentration can be detected between the two fuel groups (Table 4 and 5, and Figs. 2 and 3). Si content is lower in PV than in the mixed agropellets, all of which fairly present similar values. It also changes greatly between the two bottom ash fractions. In S1 fraction, the mean content is less than 3% for PV and ranging from 11 to 14% for the mixed fuels. The high content of SiO_2 in the form of quartz in the fraction S1 of the mixed fuels should be highlighted (Table 6). This may be the result of contamination during the harvesting of barley and corn [26]. It is worth noting that, although it is true that this quartz, like the one that is inherent to the fuel, can react with the ash elements, it is less reactive [67]. In the S2/3 fraction, the Si content is higher than that in S1, with mean values ranging from 7 to 12% for PV and from 18 to 23% for the

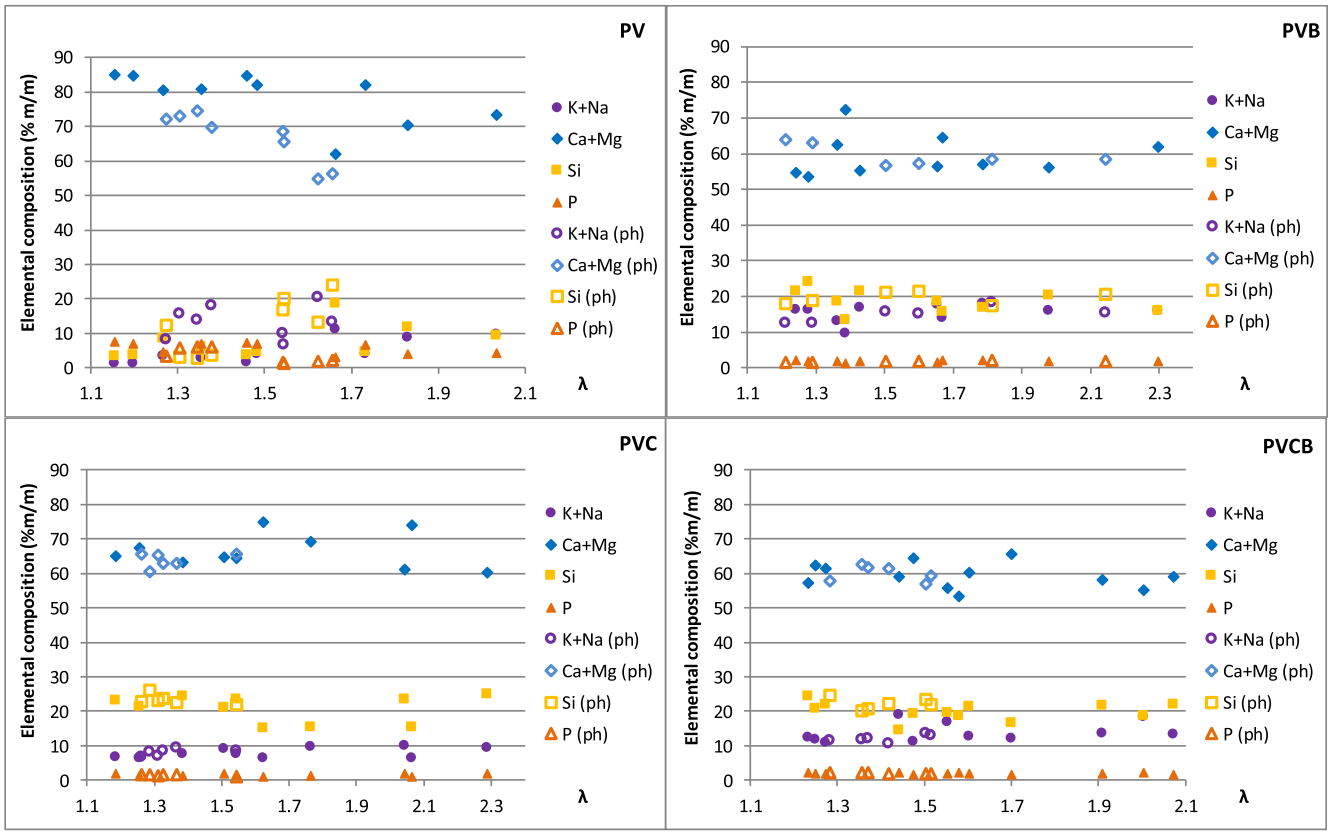

Fig. 3. Elemental composition (SEM-EDS) of S2/3 fraction of bottom ash expressed as the percentage of the total mass of measured elements (Na, Mg, Al, Si, P, S, Cl, K, Ca and Fe) against excess air ratio (λ) for PV, PVB, PVC and. Tests with (ph) and without inlet air preheating.

Table 6
Composition of S1 fraction of bottom ash (combustion tests selected).

	λ	P-XRD analysis results Crystalline matter (%)[a]									Amorphous (%)[b]
		SiO_2	$Ca_2(SiO_4)$	$Ca_2Mg(Si_2O_7)$	$K_2Ca(CO_3)_2$	$CaCO_3$	$Ca(OH)_2$	$Ca_5(PO_4)_3(OH)$	CaO	MgO	
PV	1.16	2.4			11.1	66.0		16.5		4.1	12.5
	1.46	2.3			19.1	44.2		14.0		20.3	6.1
	1.73				26.7	12.3	19.6	12.5	1.6	27.4	3.5
	2.04	9.7			17.0	31.9		15.4		26.1	20.0
	Mean	**3.6**			**18.5**	**38.6**	**4.9**	**14.6**	**0.4**	**19.5**	**10.5**
	1.34 (ph)	6.2			9.5	66.2	5.7	12.4			31.6
PVB	1.24	43.3	4.5		7.7	44.5					23.7
	1.67	24.2	7.6		13.8	54.4					19.7
	1.98	16.2	7.6		8.5	67.7					23.7
	2.30	36.1	7.4		8.5	48.1					20.6
	Mean	**30.0**	**6.8**		**9.6**	**53.7**					**21.9**
	1.29 (ph)	33.6	7.0		17.7	41.7					18.4
PVC	1.18	36.1	11.3			46.9	4.4		1.2		17.4
	1.38	28.3	15.5			46.6	7.7		2.0		15.8
	1.76	38.8	4.3			53.9			3.0		3.2
	2.29	26.0	7.5			58.1	4.7		3.6		9.9
	Mean	**32.3**	**9.7**			**51.4**	**4.2**		**2.5**		**11.6**
	1.31 (ph)	29.2	5.7			59.1	3.5		2.5		14.1
PVCB	1.23	38.0	8.8		9.9	40.2			3.1		22.4
	1.44	35.5	11.5			47.5	3.6		2.0		26.4
	1.70	33.4	12.5			50.3			3.7		28.1
	2.07	30.9	8.2		10.0	47.4			3.5		24.8
	Mean	**34.5**	**10.3**		**5.0**	**46.4**	**0.9**		**3.1**		**25.4**
	1.28 (ph)	30.8	13.2	4.8	6.4	37.4	5.6		1.9		20.1

[a] Expressed as mass percentages with regard to the total amount of crystalline matter in S1 fraction
[b] Expressed as mass percentage with regard to the total amount of S1 fraction

Table 7
Composition of S2/3 fraction of bottom ash (combustion tests selected).

	?	P-XRD analysis results Crystalline matter (%)[a]										Amorphous(%)[b]
		KCl	SiO_2	$CaSi_2$	$Ca_2(SiO_4)$	$Ca_2Mg(Si_2O_7)$	$Ca_3Mg(SiO_4)_2$	$CaCO_3$	$Ca(OH)_2$	CaO	MgO	
PV	1.16				15.3	10.3		12.1	21.9	2.8	37.6	4.6
	1.46				22.5	8.4		5.9	21.1	3	39	10.3
	1.73				15	7.6		6.9	23.1	3	44.4	23.5
	2.04		4.2		23.6	3.3		26.5	15.2	1.8	25.4	8.1
	Mean		**1.1**		**19.1**	**7.4**		**12.9**	**20.3**	**2.7**	**36.6**	**11.6**
	1.34 (ph)		1		12.1	11.1		28.3	18		29.5	24.0
PVB	1.24	3.8	2.9		39.1		32	16.3	5.8			7.1
	1.67	2.7	16.3		39.1		18.2	20	3.8			9.7
	1.98	3.2	8.1		43.3		25.3	13.7	6.4			18.3
	2.30	2.3	15.8		34.5		12.1	31.8	3.4			9.1
	Mean	**3**	**10.8**		**39**		**21.9**	**20.5**	**4.9**			**11.1**
	1.29 (ph)	2.1	20.0		34.7		22.2	17.2	3.9			17.4
PVC	1.18		4.4	3.0	29.0	30.6	15.2	10.8	7.0			11.7
	1.38		5	5.7	26.6	28.1	15.9	6.2	12.4			18.9
	1.76		3.6	4.5	31.9	31.4	18.8	9.8				15.8
	2.29		7.9	3.1	26.9	23.7	17	11.1	10.3			6.2
	Mean		**5.2**	**4.1**	**28.6**	**28.5**	**16.7**	**9.5**	**7.4**			**13.2**
	1.31 (ph)		3.1	2.7	34.1	34.2	15.6	5	5.2			10.9
PVCB	1.23		7.7		31.3	21.1	31.2	4.9	3.7			11.3
	1.44		17.3		27.7	16.3	24.8	8.9	5.1			25.9
	1.70		13.1		22.7	17.7	32.9	13.7				7.1
	2.07		2.3		31.9	28.3	25.6	4.3	7.7			18.7
	Mean		**10.1**		**28.4**	**20.9**	**28.6**	**8**	**4.1**			**15.7**
	1.28 (ph)		4.5		34	28.6	26.7	4.1	2.1			14.9

[a] Expressed as mass percentages with regard to the total amount of crystalline matter in S2/3 fraction
[b] Expressed as mass percentage with regard to the total amount of S2/3 fraction

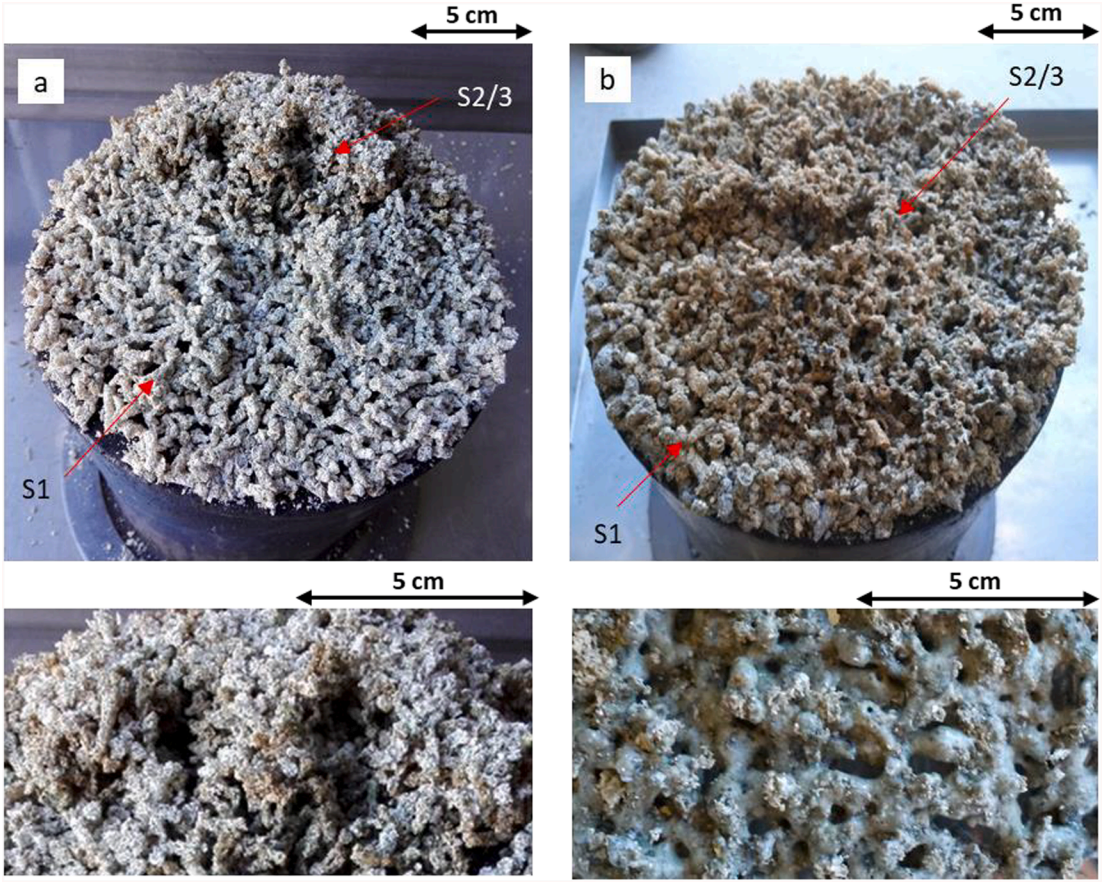

Fig. 4. Images of bottom ash after a combustion test with an enlargement of S2/3 fraction from the top of the bed: (a) PV (λ = 1.36, TC3m = 1024 °C, fraction S2/3 = 1.6%), (b) PVB (λ = 1.36, TC3m = 1079 °C, fraction S2/3 = 60.3%).

mixed agropellets. As noted, although part of the Si present in the fuel may remain unreacted (as quartz) or undergo polymorphic transformation, being present mainly in fraction S1, the formation of alkali and/or alkaline earth metal silicates is very common (Table 7).

3.2.1.4. Phosphorus. It is well-known that, in early combustion stages, some P-compounds (e.g. P_2O_5, and others subsequently formed) are highly volatile [5] and can be released from the bed. Bottom ash SEM-EDS results show that P is present in lower, but not negligible, concentrations than the previous elements: mean content around 5% for PV and 2% for the mixed agropellets. However, virtually no P-compounds (Table 6 and 7) were detected by P-XRD in bottom ash: only hydroxylapatite ($Ca_5(PO_4)_3(OH)$) was found in the S1 fraction of PV. The formation of this phosphate, which has a high melting temperature, can be explained by the higher presence of P in the PV ash. It is well known that P is predominant in the formation of compounds in combustion against Si, which has a more significant effect on PV by having a much larger P/Si ratio than mixed pellets.

Based on all this information, it is inferred that P may be present in the form of phosphates in the amorphous phase of mixed pellets as some K-phosphates melt at relatively low temperatures [26,62], even as low as K-silicates.

3.2.1.5. Chlorine and sulfur. Cl content in both S1 and S2/3 is very low (<1% and <0.1% respectively), because this element tends to form highly volatile compounds, mainly KCl (favored by the high K/Cl molar ratio of all fuels) and HCl [4] which leave the bed by vaporization at combustion temperatures. Also the concentrations of S are considerably low in both S1 and S2/3 (<2% and 1.5%, respectively), as this element tends to form gaseous SO_2/SO_3. In fact, in the P-XRD analysis no compounds with these elements were detected (except for the aforementioned KCl in the case of fraction S2/3 of the PVB).

Having discussed the results of the main chemical elements concerning ash-related problems, two main ideas can be clearly related: the high concentration of K (and, to a lesser extent, Na) compounds in the amorphous fractions (estimated on the basis of SEM-EDS and P–XRD results), and the known close relationship between sintering and the formation of alkali metal silicates and phosphates [9,68]. Based on this, it can be argued that the major differences observed in the sintering degree of bottom ash lie mainly with differences in the concentration in ash fuel preliminary analysis of K and Na on one side and Si and P on the other. Since K+Na accounts for a high percentage of the four fuels analyzed (molar ratio (K+Na)/(Si+P) > 1, except in PVC with a value of 0.92), Si+P is the limiting and determining content for sintering. This fact is reflected in a linear relationship (r=0.98, p=.015) between the molar percentage of Si+P (with regard to Na+Mg+Al+Si+P+K+Ca+Fe) in the fuel (from Table 2) and the mean sintering degree (tests without preheating, Table 3).

Si was detected in the form of Ca-(Mg)-silicates and SiO_2, which is practically absent from PV. The former compounds come partially from secondary reactions of Ca and Mg with the initially molten compounds. K-silicates and K-phosphates, which were not detected but are undoubtedly present in the amorphous phase, explain the greater sintering degree attested for the mixed agropellets, since the presence of Si in fuels with an herbaceous component is higher.

Furthermore, despite differences in sintering degree in the bottom ash of the mixed agropellets, no clear differences that could account for this behavior were found in the P-XRD results. The crystalline phases detected are almost identical and are present in similar concentrations. In addition, the amorphous fraction does not seem to be affected by changes in the sintering degree.

Finally, comparing the mean bottom ash composition detected by SEM-EDS (as a weighted average[2] of the fractions S1 and S2/3 of all tests) and that of the fuel ash obtained in the preliminary analysis (extracted from Table 2), a significant and complementary result can be inferred. This comparison is presented in Fig. 5, where SEM-EDS results are plotted as the average of concentrations for the tested range of λ.

Some differences can be detected between both analysis owing to the different ashing conditions, mainly combustion temperature, but also residence time, λ and turbulence. At any rate, these differences affected all fuels in a similar way in terms of the relative position of the three groups of elements in the plot. In this way, K+Na group contents are lower in the SEM-EDS analysis than the concentrations detected in the ash fuel preliminary analysis because these elements tend to evaporate from the bed as a result of the high-temperature conditions in the reactor. The Ca+Mg group is still the most abundant; its concentration (as detected by SEM-EDS) is higher than in the preliminary analysis of the ash fuel, as alkaline earth metals do not vaporize [5] or do so only in very small proportions [69]. As for Si, like the Ca+Mg, the proportion of this element in the ash is greater after the tests than in the ash fuel preliminary analysis since Si forms compounds (silicates, aluminosilicates and oxides) that remain solid regardless of combustion temperatures [5,26].

3.2.2. Influence of operating conditions

The two operating conditions analyzed are Ta and λ. Based on the results provided by the P-XRD, the impact of λ on the composition of the bottom ash remains unclear because no correlation with either the percentage of the detected phases or the percentage of amorphous phase in any of the fuels (four tests without preheating air analyzed for each fuel; see Table 6 and 7). This may be due to the relatively small difference between the combustion temperatures for each fuel (<300 °C in TC3m; see Table 3); other studies in which the temperature range was wider (e.g., [17]) have attested greater compositional differences, suggesting that the amorphous fraction increases with higher temperatures. It is also not possible to find significant differences in the P-XRD results between the tests with preheating (one test analyzed for each fuel) and without preheating. Therefore, in this section only the SEM-EDS results are used to analyze the influence of the two parameters noted above.

3.2.2.1. Influence of Ta. Regarding the effect of inlet air temperature, to correctly analyze the results it is first necessary to establish the variations in air velocity and combustion temperature between the

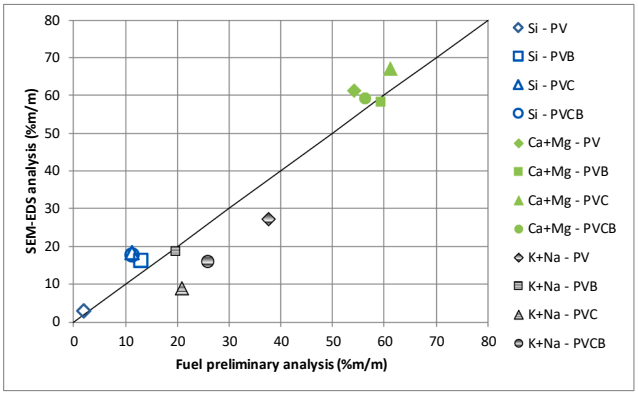

Fig. 5. Concentration in ash fuel preliminary analysis (obtained from Table 2) versus mean bottom ash composition (S1+S2/3) from SEM-EDS.[3]

[2] The percentages of fractions S1 and S2/3 are presented in [52].

[3] In both cases, mass percentages of each element with respect to Na+Mg+Al+Si+P+K+Ca+Fe.

experimental tests with and without preheating (see Table 3). In preheated tests, air velocity in the bed increased compared to tests without preheating with a similar λ range (in the order of 40% on average for each fuel), due to both the increase in the specific volume of the air and the ignition rate [52], but this did not lead to significant temperature increases in TC3m for the mixed agropellets (in the order of 20 °C on average for each fuel) while leading to a temperature decrease for PV (approximately 100 °C on average).

As illustrated by Table 4 and 5, and Figs. 2 and 3, no significant effect on the concentration of the main elements present in the ash resulted from preheating (except in the case of S2/3 for PV; however, due to the already noted low percentage that this fraction represents, this is not highly relevant). Only, in the case of the mixed agropellets a slight increase in the percentage of Si and a slight decrease in the proportion of K+Na (especially in PVB and PVCB) in the preheated tests is worth mentioning. The reason may be that Si in presence of K+Na has a tendency to form sintering compounds, being less affected by the increase in air velocity (entrainment), whereas K+Na may be affected by an increase in vaporization and entrainment (as K+Na is partially present in small-particle compounds).

3.2.2.2. Influence of λ. Concerning the effects of excess air, it is once again necessary to take into account how it affected combustion temperature and air velocity (see Table 3 and [52]). When λ increased, TC3m values decreased (in the order of 250 °C for the mixed agropellets and in the order of 175 °C for PV in the tested λ range, tests without preheating) and air velocity in the bed increased (between 15 and 25% for the mixed agropellets and in the order of 30% for PV in the tested λ range, tests without preheating).

First, concerning the influence of λ on bottom ash, it was observed that, for PV, increased λ led to a significant decrease in bottom ash [52]. The low quantity of bottom ash in PV, as well as its reduction with increased λ, could be related to a high particle entrainment. However, in the mixed agropellets the proportion of bottom ash was not significantly affected by increased λ [52]. One possibility to explain could be that, within the combustion temperature (TC3m) and air velocity ranges tested (see Table 3), the expected level of ash fractionation was reached, leading to the bottom ash fraction remaining on the grate, while the more volatilized components and fine particles were released. However, other possible explanation could be that the decrease in the quantity of volatilized ash (due to lower combustion temperature) was offset by the increase in ash entrainment caused by higher air velocity.

Using the results of the SEM-EDS to interrogate these possible explanations, it can be observed that variations in the composition of bottom ash (both in S1 and S2/3) with different λ (Figs. 2 and 3) are of little significance. Nevertheless, it must be considered that these are percentages of elements from fractions (S1 and S2/3) that also vary depending on λ.

To analyze the results taking this fact into account, the quantity of each element in fractions S1 and S2/3 is estimated considering a proportion of 1 kg of Ca+Mg+Si+P+Al+Fe+K+Na per 2 kg of the ash compounds which are typically formed in combustion [53]. Thus, by multiplying the concentration of each element in the corresponding fraction ($kg_{element\_i}/kg_{Ca+Mg+Si+P+Al+Fe+K+Na}$, Figs. 2 and 3) by the percentage represented by each fraction (from [52]) and dividing by 2 ($kg_{ash}/kg_{Ca+Mg+Si+P+Al+Fe+K+Na}$), the quantity of each element in each fraction per unit of ash introduced with the fuel is obtained ($kg_{element\_i}/kg_{ash}$). To take into consideration the specific characteristics of each fuel, this magnitude is subsequently multiplied by ash concentration and divided by the HHV (Table 1), the result being the mass of each element in each fraction per unit of energy introduced with the fuel:

$$\text{Elemental mass in fraction X per unit of energy} = \frac{\text{Elemental composition (SEM-EDS)}\cdot\%\ \text{Fraction X}\cdot\text{Ash}_{fuel}}{2\cdot\text{HHV}_{fuel}}$$

Where:

- *Elemental composition (SEM-EDS)*: elemental composition yielded by SEM-EDS, expressed as a percentage of the total mass of measured elements (Na, Mg, Al, Si, P, S, Cl, K, Ca and Fe, see Figs. 2 and 3).
- *% Fraction X*: mass percentage of S1 or S2/3 (see [52]).
- Ash_{fuel}: mass percentage of ash in the fuel (d.b., see Table 1).
- HHV_{fuel}: high heating value of the fuel (d.b. at p=constant, see Table 1).

From this formula, the quantity of each element ($g_{element\_i}/GJ$) as a function of λ is shown in Figs. 6 and 7. These figures also show the trend lines, which are subsequently analyzed from the point of view of their statistical relevance (Pearson's coefficient and p-values) in Table 8.

As can be seen in Table 8, most linear correlations are statistically relevant. Those that are not, correspond to data series of relatively low concentration and/or practically insensitive to the variation of λ.

It is observed that in all the mixed agropellets an increase in λ results in an increase of the amount of Si retained in S1 fraction (by a factor of 3–4 in the range of λ analyzed). This behavior is partially offset by a decrease in the amount of Si retained in fraction S2/3 (approximately half); both fractions yield very similar values for high λ (in the order of 100 g/GJ in all the mixed agropellets). For all these fuels, it can be observed that the amount of Si that remains as bottom ash (the sum of the fractions S1 – Fig. 6 – and S2/3 – Fig. 7) decreases with increasing λ, which can only be a consequence of greater entrainment, since Si is refractory [5,26] and consequently does not vaporize in the temperature ranges considered. Regarding PV, it is not possible to determine a correlation between retained Si and λ either in S1 or in S2/3 (see Table 8).

Concerning Ca+Mg, which are elements that can be considered practically refractory, in the mixed agropellets the behavior with increasing λ is similar to that of Si in both S1 and S2/3, although in the case of bottom ash (S1+S2/3) no clear trend can be attested, increasing slightly in PVB and PVC, and decreasing slightly in PVCB. In the case of PV, the amount of these elements decreases with increasing λ in both S1 and S1+S2/3, which is indicative of substancial entrainment.

Due to the low quantity of P, despite having low p-values in some correlations, no clear conclusions for this element can be drawn.

In the mixed agropellets, with increasing λ, the amount of K+Na retained in the S1 increases significantly in PVB and PVCB (in the case of PVC, no trend can be attested, as the correlations are not statistically relevant), whereas in S2/3 it decreases for PVB, but to a lesser extent (in the cases of PVC and PVCB, the correlations are not statistically significant). Overall, in terms of bottom ash, a slight increase in these elements ensues with increasing λ. That is, despite the greater entrainment, which also affects the K and Na compounds, an increase in these two elements is observed, which can only be due to a decrease in vaporization. The case of PV is different, since a certain decrease in the amount of K+Na is observed in S1 (although there is insufficient evidence to conclude that there is a significant relationship because p-value is somewhat greater than .05) and remains fairly constant (yielding very low values) in the S2/3 fraction. This behavior confirms the importance of the entrainment phenomenon in this fuel, which is not compensated for by the possible decrease in vaporization caused by the decrease in combustion temperatures.

Therefore, the analysis of the influence of increasing λ on the mixed agropellets reveals a decrease in Si (the most representative of refractory elements) concentration in bottom ash, which is related to increased entrainment as air velocity in the bed increases. In contrast, it also

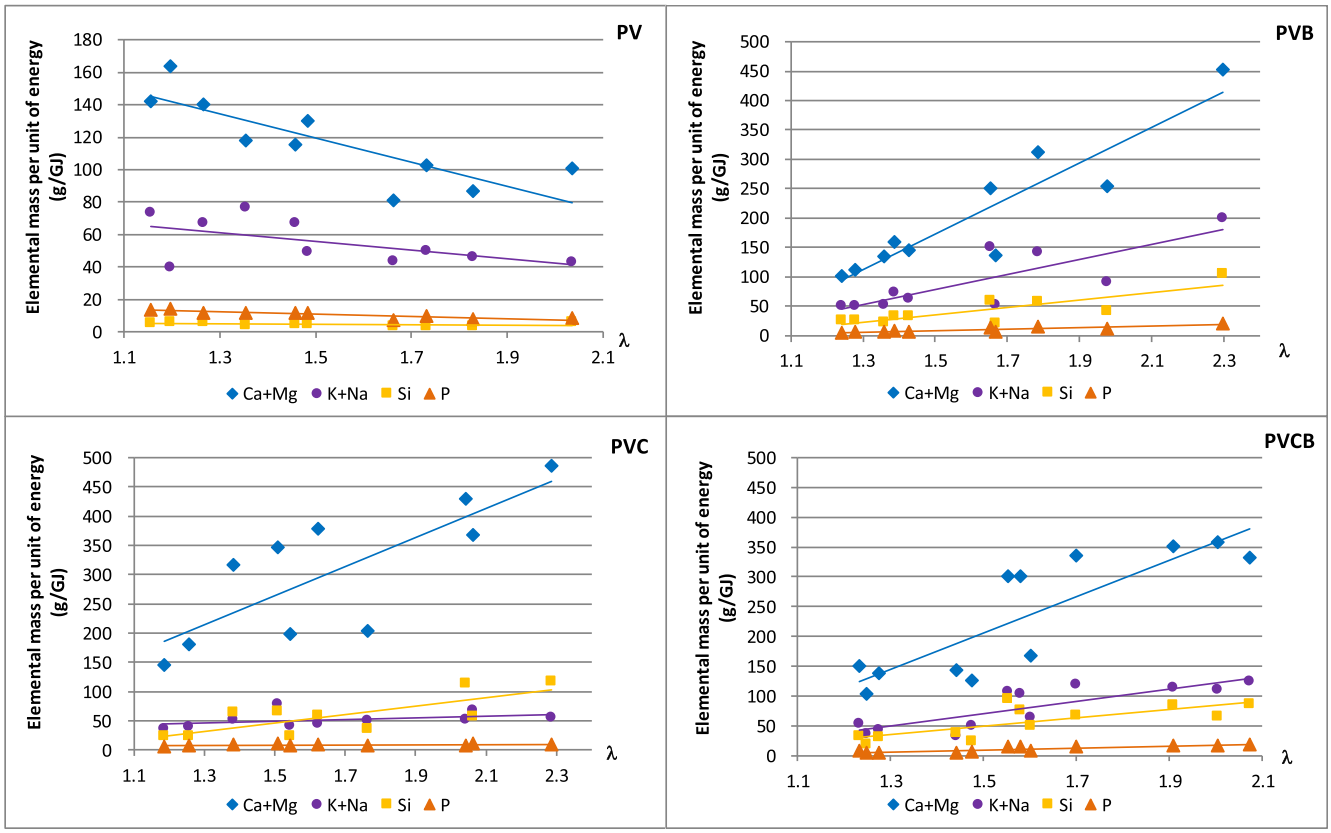

Fig. 6. Si, K+Na, Ca+Mg and P in S1 fraction (g per GJ of fuel, HHV reference) against λ.

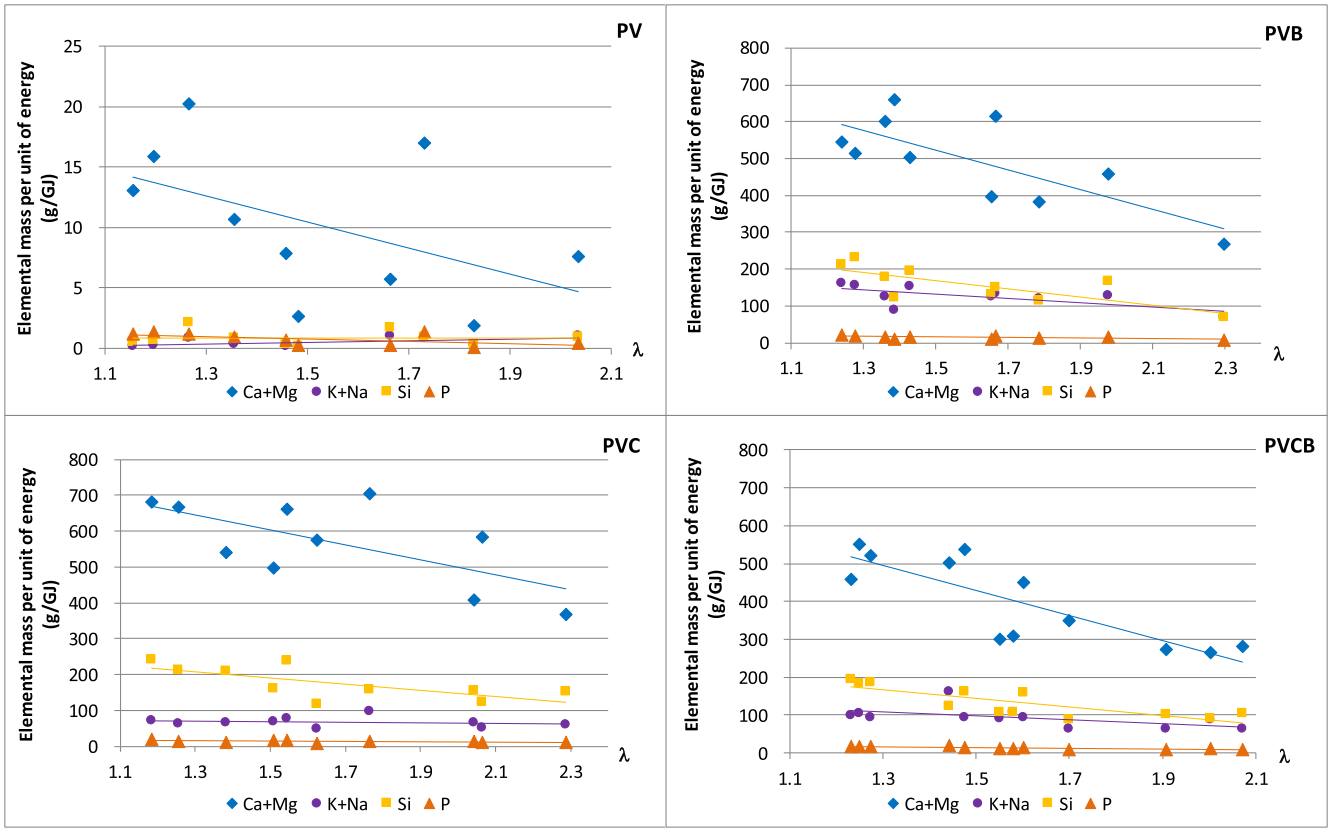

Fig. 7. Si, K+Na, Ca+Mg and P in S2/3 fraction (g per GJ of fuel, HHV reference) against λ.

Table 8
Pearson's coefficient (r) and p-values (p) of the correlations between the concentrations of each element and ? (Figs. 6 and 7).

		Ca+Mg		K+Na		Si		P	
		r	p	r	p	r	p	r	p
S1	**PV**	-.823	.003	-.572	.084	-.378	>.1	-.867	.001
	PVB	.918	<.001	.808	.005	.824	.003	.864	.001
	PVC	.784	.007	.442	>.1	.764	.001	.350	>.1
	PVCB	.850	<.001	.834	.001	.747	.008	.866	<.001
S2/3	**PV**	-.505	>.1	-.482	>.1	.035	>.1	-.588	.073
	PVB	-.753	.012	-.653	.041	-.763	.001	-.616	.058
	PVC	-.659	.038	-.227	>.1	-.697	.025	-.527	>.1
	PVCB	-.826	.002	-.548	.081	-.811	.002	-.823	.002

suggests an increase in the amount of K+Na, which is related to a decrease in vaporization as combustion temperature decreases; concerning these elements, this effect is more important than the entrainment effect. Thus, it can be concluded that, with the mixed agropellets, bottom ash is little affected by λ, due to two opposing phenomena (entrainment and vaporization), the effects of which are of a similar magnitude in the tests carried out when varying λ, although it was not possible to quantify it. In the case of PV, where bottom ash proportion decreases for higher λ, entrainment is the dominant effect which is reflected in a clear decrease in all the elements.

To highlight the influence of excess air on the sintering degree, Fig. 8 presents this parameter as a function of the molar percentage of Si+P in the fuel for the means of three selected λ ranges (λ<1.4, 1.4<λ<1.8 and λ>1.8).

First, as mentioned for the mean values of all tests, there is also a clear direct correlation between sintering degree and Si+P concentration in all ranges of λ (r=.97, p=.028 for λ<1.4; r=.99, p=.01 for1.4-<λ<1.8 and r=.99, p=.014 for λ>1.8). It should be noted that this direct correlation occurs in the fuels analyzed in this study given their already mentioned high K+Na content and significant Si+P content (with high molar ratio (K+Na)/(Si+P)). In other cases, the trends may be very different and even contrary to the one observed here, such as when Si is clearly predominant over K+Na or when P and Ca+Mg content is really high. In these two given situations, sintering phenomenon can be reduced by the absence of K-silicates and the fixation of K in K-Ca-phosphates [70] respectively, as is reflected from the analysis of the ternary diagrams presented, among others, by [17] and [71].

With respect to the influence of λ, it can be seen in Fig. 8 that, due to the decrease in combustion temperature that it produces, the greater the excess air, the lower the sintering degree, an effect that tends to increase with greater Si+P concentrations. Therefore, in the case of PVB operating at low λ (<1.4), switching to high λ (>1.8) means reducing the sintering degree by more than 20 percentage points in the tests carried out, the same order of magnitude that would have resulted from using a fuel with a Si+P content around 4.5 percentage points lower. However,

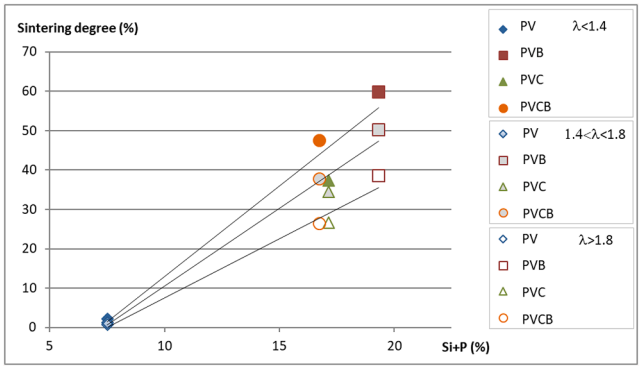

Fig. 8. Mean sintering degree of bottom ash versus Si+P concentration in fuel preliminary analysis (molar percentage with respect to Na + Mg + Al + Si + P + K + Ca + Fe, from Table 2 for three λ ranges.

in the case of PV, λ variation is irrelevant in terms of sintering degree. These results reinforce the idea that sintering is affected by both fuel composition and operational parameters.

4. Conclusions

The results of the SEM-EDS and P-XRD analysis have confirmed that the different behavior in terms of bottom ash proportion and sintering degree of four tested agropellets are closely related to the formation of alkali metal silicates and, to a lesser extent, phosphates. As the percentage of K+Na is very high in the four fuels under analysis (molar ratio (K+Na)/(Si+P) over 0.9 in all cases), Si+P is the limiting and determining content as far as sintering is concerned, and thus a direct correlation between Si+P concentration in the fuel and sintering degree can be attested.

Alkaline earth metals are predominant in bottom ash in all cases, forming mainly carbonates in S1 and silicates in S2/3. However, neither SEM-EDS nor P-XRD analysis have clearly presented relevant differences between the bottom ash composition of the three mixed agropellets that can explain the varying sintering degrees attested.

Regarding the influence of operating conditions, only small variations in the concentration of the main chemical elements present in both S1 and S2/3 fractions have been detected when varying Ta and λ in the tested range. Nevertheless, since the composition of both fractions is different and their proportions vary with λ, the analysis of SEM-EDS results of mixed agropellets have pointed to the opposite effects of entrainment and vaporization, which explained why bottom ash proportion seemed not to be influenced by excess air in the analyzed range of λ [52]. For these fuels, operating with high levels of excess air (which means a higher air velocity in the bed and a lower combustion temperature) leads bottom ash to present a lower sintering degree and therefore fewer operational problems, increasing entrainment but decreasing vaporization. However, higher λ could affect the volume of particles expelled by the chimney and lead to a decrease in thermal efficiency. In any case, these negative effects can be greatly reduced by the use of an oversized particle capture system and condensing boilers, respectively. In fuels that present a low sintering degree, as with PV, SEM-EDS results have confirmed that entrainment is the dominant effect, so that the increase in λ implies very high entrainment of solid particles, with the resulting negative effect on deposition, erosion and chimney emissions. Due to this fact, and keeping in mind that no significant advantages in terms of sintering are otherwise forthcoming (as this is no longer a serious problem), operating with high λ values with this type of fuels is not recommended.

However, based solely on the information of bottom ash it is not possible to determine the partitioning behavior of each element (percentage retained in the bed, released by entrainment and by vaporization), nor quantify the influence of Ta and λ (air velocity and combustion temperature) in ash entrainment and vaporization. For this, it is necessary to jointly analyze the behavior of the bottom ash and the part that leave the bed (closely related to the deposition, discussed in [52]). This will be done at a later stage of the investigation.

CRediT authorship contribution statement

Javier Royo: Conceptualization, Methodology, Formal analysis, Investigation, Writing - original draft, Writing - review & editing, Visualization, Supervision, Project administration, Funding acquisition. **Paula Canalís:** Conceptualization, Methodology, Formal analysis, Investigation, Writing - original draft, Writing - review & editing, Visualization, Project administration. **David Quintana:** Conceptualization, Methodology, Formal analysis, Investigation, Writing - original draft, Writing - review & editing, Visualization.

Declaration of Competing Interest

The authors declare that they have no known competing financial interests or personal relationships that could have appeared to influence the work reported in this paper.

Acknowledgments

The authors greatly acknowledge the Spanish Ministry of Science and Innovation and the Spanish Ministry of Universities for funding the project "MHWPellet: Mixed pellets based on agricultural crops residues (herbaceous and woody) for their use in the residential sector: optimization of their composition and conversion parameters" (ref. ENE2015-68809-R (MIMECO/FEDER, UE)).

The authors also would like to acknowledge the use of*Servicio General de Apoyo a la Investigación-SAI, Universidad de Zaragoza*.

References

[1] Scarlat N, Dallemand J-F, Monforti-Ferrario F, Nita V. The role of biomass and bioenergy in a future bioeconomy: Policies and facts. Environ Dev 2015;15:3–34.
[2] Bozell JJ, Black SK, Myers M, Cahill D, Miler WP, Park S. Solvent fractionation for renewable woody feedstocks: Organoslv generation of biorefinery process streams for the production of biobased chemicals. Biomass Bioenergy 2011;35(10):4197–208.
[3] Scarlat N, Dallemand J-F, Monforti-Ferrario F, Banja M, Motola V. Renewable energy policy framework and bioenergy contribution in the European Union – An overview from National Renewable Energy Action Plans and Progress Reports. Renew Sustain Energy Rev 2015;51:969–85.
[4] Zeng T, Weller N, Pollex A, Lenz V, Nelles M. Blended biomass pellets as fuel for small scale combustion appliances: Influence on gaseous and total particulate matter emissions and applicability of fuel indices. Fuel 2016;184(689):700.
[5] Boström D, Skoglund N, Grimm A, Boman C, Öhman M, Broström M, et al. Ash transformation chemistry during combustion of biomass. Energy Fuels 2012;26(1):85–93.
[6] Díaz-Ramírez M, Sebastián F, Royo J, Rezeau A. Influencing factors on NOX emission level during grate conversion of three pelletized energy crops. Appl Energy 2014;115:360–73.
[7] Johansson LS, Leckner Bo, Gustavsson L, Cooper D, Tullin C, Potter A. Emission characteristics of modern and old-type residential boilers fired with wood logs and wood pellets. Atmos Environ 2004;38(25):4183–95.
[8] Obernberger I, Biedermann F, Widmann W, Riedl R. Concentrations of inorganic elements in biomass fuels and recovery in the different ash fractions. Biomass Bioenergy 1997;12(3):211–24.
[9] Wierzbicka A, Lillieblad L, Pagels J, Strand M, Gudmundsson A, Gharibi A, et al. Particle emissions from district heating units operating on three commonly used biofuels. Atmos Environ 2005;39(1):139–50.
[10] Wiinikka H, Gebart R, Boman C, Boström D, Öhman M. Influence of fuel ash composition on high temperature aerosol formation in fixed bed combustion of woody biomass pellets. Fuel 2007;86(1-2):181–93.
[11] Wiinikka H, Gebart R. Experimental investigations of the influence from different operating conditions on the particle emissions from a small-scale pellets combustor. Biomass Bioenergy 2004;27(6):645–52.
[12] Brunner T., Obernberger I., Scharler R. Primary measures for low-emission residential wood combustion - Comparison of old with optimised modern systems. Proceedings of 17th European Biomass Conference and Exhibition, Hamburg: Germany; 2009, 1319-1328.
[13] OBERNBERGER I, BRUNNER T, BARNTHALER G. Chemical properties of solid biofuels–significance and impact. Biomass Bioenergy 2006;30(11):973–82.
[14] Díaz-Ramírez M, Boman C, Sebastián F, Royo J, Xiong S, Boström D. Ash Characterization and Transformation Behavior of the Fixed-Bed Combustion of Novel Crops: Poplar, Brassica, and Cassava Fuels. Energy Fuels 2012;26(6):3218–29.
[15] Díaz-Ramírez M, Sebastian F, Royo J, Rezeau A. Combustion requirements for conversion of ash-rich novel energy crops in a 250 kWth multifuel grate fired system. Energy 2012;46(1):636–43.
[16] Díaz-Ramírez M, Frandsen FJ, Glarborg P, Sebastián F, Royo J. Partitioning of K, Cl, S and P during combustion of poplar and brassica energy crops. Fuel 2014;134:209–19.
[17] Vassilev SV, Baxter D, Vassileva CG. An overview of the behaviour of biomass during combustion: Part II. Ash fusion and ash formation mechanisms of biomass types. Fuel 2014;117:152–83.
[18] Zhu Y, Tan H, Niu Y, Wang X. Experimental study on ash fusion characteristics and slagging potential using simulated biomass ashes. J Energy Inst 2019;92(6):1889–96.
[19] Fernández MJ, Mediavilla I, Barro R, Borjabad E, Ramos R, Carrasco JE. Sintering reduction of herbaceous biomass when blended with woody biomass: predictive and combustion tests. Fuel 2019;239:1115–24.
[20] Rodriguez JL, Álvarez X., Valero E., Ortiz L., de la Torre-Rodríguez N., Acuña-Alonso C. Influence of ashes in the use of forest biomass as source of energy. Fuel, 2021: 283 Doi: 10.1016/j.fuel.2020.119256.
[21] Lachman J, Baláš M, Lisý M, Lisá H, Milčák P, Elbl P. An overview of slagging and fouling indicators and their applicability to biomass fuels. Fuel Process Technol 2021;217:106804. https://doi.org/10.1016/j.fuproc.2021.106804.
[22] Vassilev SV, Baxter D, Andersen LK, Vassileva CG, Morgan TJ. An overview of the organic and inorganic phase composition of biomass. Fuel 2012; 94: 1–33. Doi: 10.1016/j.fuel.2011.09.030.
[23] Vassilev SV, Baxter D, Andersen LK, Vassileva CG. An overview of the chemical composition of biomass. Fuel 2010;89(5):913–33.
[24] Glarborg P, Marshall P. Mechanism and modeling of the formation of gaseous alkali sulfates. Combust Flame 2005;141(1-2):22–39.
[25] Garba MU, Ingham DB, Ma L, Porter RTJ, Pourkashnian M, Tan HZ, et al. Prediction of Potassium Chloride Sulfation and Its Effect on Deposition in Biomass-Fired Boilers. Energy Fuels 2012;26(11):6501–8.
[26] Niu Y, Tan H, Hui S. Ash-related issues during biomass: Alkali-induced slagging, silicate melt-induced slagging (ash fusion), agglomeration, corrosion, ash utilization, and related countermeasures. Prog Energy Combust Sci 2016;52:1–61.
[27] Capablo J. Formation of alkali salt deposits in biomass combustion. Fuel Process Technol 2016;153:58–73.
[28] Carvalho L, Wopienka E, Pointner C, Lundgren J, Verma VK, Haslinger W, et al. Performance of a pellet boiler fired with agricultural fuels. Appl Energy 2013;104:286–96.
[29] Wang L, Skjevrak G, Hustad JE, Grønli M, Skreiberg Ø. Effects of Additives on Barley Straw and Husk Ashes Sintering Characteristics. Energy Procedia 2012;20:30–9.
[30] Sippula O, Hytönen K, Tissari J, Raunemaa T, Jokiniemi J. Effect of Wood Fuel on the Emissions from a Top-Feed Pellet Stove. Energy Fuels 2007;21(2):1151–60.
[31] Houshfar E, Lovas T, Skreiberg O. Experimental Investigation on NOX Reduction by Primary Measures in Biomass Combustion: Straw, Peat, Sewage Sludge, Forest Residues and Wood Pellets. Energies 2012;5(2):270–90.
[32] Boström D, Grimm A, Boman C, Björnbom E, Öhman M. Influence of kaolin and calcite additives on ash transformations in small-scale combustion of oat. Energy & Fuel 2009;23(10):5184–90.
[33] Lindström E, Sandström M, Boström D, Öhman M. Slagging Characteristics during Combustion of Cereal Grains Rich in Phosphorus. Energy Fuels 2007;21(2):710–7.
[34] Vassilev SV, Baxter D, Andersen LK, Vassileva CG. An overview of the composition and application of biomass ash. Part 1. Phase–mineral and chemical composition and classification. Fuel 2013;105:40–76.
[35] Zeng T, Pollex A, Weller N, Lenz V, Nelles M. Blended biomass pellets as fuel for small scale combustion appliances: Effect of blending on slag formation in the bottom ash and pre-evaluation options. Fuel 2018;212:108–16.
[36] Rodriguez JL, Álvarez X, Valero E, Ortiz L, de la Torre-Rodríguez N, Acuña-Alonso C. Design of solid biofuels blends to minimize the risk of sintering in biomass boiler. J Energy Inst 2020;93:2409–14.
[37] Míguez JL, Porteiro J, Behrendt F, Blanco D, Patiño D, Dieguez-Alonso A. Review of the use of additives to mitígate operational problems associated with the combustion of biomass with high content in ash-forming species. Renew Sustain Energy Rev 2021;141:110502. https://doi.org/10.1016/j.rser.2020.110502.
[38] Becidan M, Houshfar E, Khalil RA, Skreiberg Ø, Løvås T, Sørum L. Optimal Mixtures to Reduce the Formation of Corrosive Compounds during Straw Combustion: A Thermodynamic Analysis. Energy Fuels 2011;25(7):3223–34.
[39] Khor A, Ryu C, Yang Y-B, Sharifi VN, Swithenbank J. Straw combustion in a fixed bed combustor. Fuel 2007;86(1-2):152–60.
[40] Magdziarz A, Dalai AK, Koziński JA. Chemical composition, character and reactivity of renewable fuel ashes. Fuel 2016;176:135–45.
[41] Pérez-Orózco R, Patiño D, Porteiro J, Rico JJ. The effect of primary measures for controlling biomass bed temperature on PM emission through analysis of the generated residues. Fuel, 2020: 280 Doi: 10.1016/j.fuel.2020.118702.
[42] Fernández Llorente MJ, Escalada Cuadrado R, Murillo Laplaza JM, Carrasco García JE. Combustion in bubbling fluidised bed with bed material of limestone to reduce the biomass ash agglomeration and sintering. Fuel 2006;85(14-15):2081–92.
[43] Knudsen JN, Jensen PA, Dam-Johansen K. Transformation and release to the gas phase of Cl, K, and S during combustion of annual biomass. Energy Fuels 2004;18(5):1385–99.
[44] van Lith SC, Alonso-Ramírez V, Jens PA, Frandsen FJ, Glarborg P. Release to the gas phase of inorganic elements during wood combustion. Part 1: Development and evaluation of quantification methods. Energy Fuels 2006;20(3):964–78.
[45] Theis M, Skrifvars B-J, Hupa M, Tran H. Fouling tendency of ash resulting from burning mixtures of biofuels. Part 1: deposition rates. Fuel 2006;85(7-8):1125–30.
[46] Li G, Li S, Xu X, Huang Q, Yao Q. Dynamic behavior of biomass ash deposition in a 25 kW one-dimensional down-fired combustor. Energy Fuels 2014;28(1):219–27.

[47] Zhou H, Jensen A, Glarborg P, Kavaliauskas A. Formation and reduction of nitric oxide in fixed-bed combustion of straw. Fuel 2006;85(5-6):705–16.
[48] Ryu C, Yang YB, Khor A, Yates NE, Sharifi VN, Swithenbank J. Effect of fuel properties on biomass combustion: Part I. Experiments – fuel type, equivalence ratio and particle size. Fuel 2006;85(7-8):1039–46.
[49] Porteiro J, Patiño D, Collazo J, Granada E, Moran J, Miguez JL. Experimental analysis of the ignition front propagation of several biomass fuels in a fixed-bed combustor. Fuel 2010;89(1):26–35.
[50] Regueiro A, Patiño D, Granada E, Porteiro J. Experimental study on the fouling behaviour of an underfeed fixed-bed biomass combustor. Appl Therm Eng 2017;112:523–33.
[51] Erić A, Nemoda S, Komatina M, Dakić D, Repić B. Experimental investigation on the kinetics of biomass combustion in vertical tube reactor. J Energy Inst 2019;92(4):1077–90.
[52] Royo J, Canalís P, Quintana D, Díaz-Ramírez M, Sin A, Rezeau A. Experimental study on the ash behaviour in combustion of pelletized residual agricultural biomass. Fuel 2019;239:991–1000.
[53] Royo J, Canalís P, Quintana D. Chemical study of fly ash deposition in combustion of pelletized residual agricultural biomass. Fuel 2020;268:117–228.
[54] Canalís-Martínez P, Royo J, Quintana D, Rezeau A. Present and future of mixed pellets based on agricultural crops residues (herbaceous and woody) for their use in the residential sector (MHWPELLET PROJECT). Proceedings of the 26TH European Biomass Conference and Exhibition, 14-17 May 2018, Copenhagen, Denmark.
[55] Öhman M, Boman C, Hedman H, Nordin A, Boström D. Slagging tendencies of wood pellet ash during combustion in residential pellet burners. Biomass Bioenergy 2004;27(6):585–96.
[56] Vassilev SV, Vassileva CG. Methods for characterization of composition of fly ashes from coal-fired power stations: A critical overview. Energy Fuels 2005;19:1084–98.
[57] Deng L, Jin Xi, Long J, Che D. Ash deposition behaviors during combustion of raw and water washed biomass fuels. J Energy Inst 2019;92(4):959–70. https://doi.org/10.1016/j.joei.2018.07.009.
[58] Imran M, Khan A. Characterization of Agricultural Waste Sugarcane Bagasse Ash at 11000C with various hours. Mater Today: Proc 2018;5:3346–52.
[59] Liu Y, He Y, Wang Z, Xia J, Wan K, Whiddon R, et al. Characteristics of alkali species release from a burning coal/biomass blend. Appl Energy 2018;215:523–31.
[60] Llorente MJF, Arocas PD, Nebot LG, García JEC. The effect of the addition of chemical materials on the sintering of biomass ash. Fuel 2008;87(12):2651–8.
[61] Wang L, Skreiberg Ø, Becidan M. Investigation of additives for preventing ash fouling and sintering during barley straw combustion. Appl Therm Eng 2014;70(2):1262–9.
[62] Zevenhoven M, Yrjas P, Skrifvars B-J, Hupa M. Characterization of ash-forming matter in various solid fuels by selective leaching and its implications for fluidized-bed combustion. Energy Fuels 2012;26(10):6366–86.
[63] Vassilev SV, Baxter D, Vassileva CG. An overview of the behaviour of biomass during combustion: Part I. Phase-mineral transformations of organic and inorganic matter. Fuel 2013;112:391–449.
[64] Thy P, Jenkins BM, Lesher CE. High-Temperature Melting Behavior of Urban Wood Fuel Ash. Energy Fuels 1999;13:839–50.
[65] Vamvuka D, Zografos D. Predicting the behaviour of ash from agricultural wastes during combustion. Fuel 2004;83(14-15):2051–7.
[66] THY P, JENKINS B, GRUNDVIG S, SHIRAKI R, LESHER C. High temperature elemental losses and mineralogical changes in common biomass ashes. Fuel 2006;85(5-6):783–95.
[67] Vassileva CG, Vassilev SV. Behaviour of inorganic matter during heating of Bulgarian coals 1. Lignites. Fuel Processing Technology 2005;86:1297–333.
[68] Sommersacher P, Brunner T, Obernberger I. Fuel indexes: A novel method for the evaluation of relevant combustion properties of new biomass fuels. Energy Fuels 2012;26(1):380–90.
[69] Okuno T, Sonoyama N, Hayashi J-i, Li C-Z, Sathe C, Chiba T. Primary release of alkali and alkaline earth metallic species during the pyrolysis of pulverized biomass. Energy Fuels 2005;19(5):2164–72. https://doi.org/10.1021/ef050002a.
[70] Wang Q, Han K, Wang J, Gao J, Lu C. Influence of phosphorous based additives on melting characteristics during combustion of biomass briquette fuel. Renewable Energy 2017;113:428–37.
[71] Näzelius I-L, Boström D, Rebbling A, Boman C, Öhman M. Fuel indices for estimation of slagging of phosphorus-poor biomass in fixed bed combustion. Energy Fuels 2017;31(1):904–15.